Journal of General Virology (2008), **89**, 2437–2446 **DOI** 10.1099/vir.0.2008/003897-0

Activation of the ERK signal transduction pathway by Epstein–Barr virus immediate-early protein Rta

Yu-Hsiu Lee,[1] Ya-Fang Chiu,[2] Wen-Hung Wang,[2] Li-Kwan Chang[3] and Shih-Tung Liu[2]

Correspondence
Shih-Tung Liu
cgliu@mail.cgu.edu.tw

[1]Institute of Microbiology and Immunology, National Yang-Ming University, 155 Linong Street Section 2, Taipei 112, Taiwan, ROC

[2]Molecular Genetics Laboratory, Department of Microbiology and Immunology, Chang-Gung University, 259 Wen-Hua 1st Road, Kwei-Shan, Taoyuan 333, Taiwan, ROC

[3]Institute of Microbiology and Biochemistry, National Taiwan University, 1 Roosevelt Road Section 4, Taipei 106, Taiwan, ROC

Received 7 May 2008
Accepted 9 June 2008

BRCA1-associated protein 2 (BRAP2) is known to interact with the kinase suppressor of Ras 1 (KSR1), inhibiting the ERK signal transduction cascade. This study found that an Epstein–Barr virus (EBV) immediate-early protein, Rta, is a binding partner of BRAP2 in yeast and confirmed the binding *in vitro* by a glutathione *S*-transferase pull-down assay and *in vivo* by co-immunoprecipitation in 293(maxi-EBV) cells. Binding studies also showed that Rta and KSR1 interacted with the C-terminal 202 aa region in BRAP2. Additionally, Rta appeared to prevent the binding of KSR1 to BRAP2, activating the ERK signal transduction pathway and the transcription of an EBV immediate-early gene, *BZLF1*. Activation of the ERK signal transduction pathway by Rta may be critical for the maintenance of the lytic state of EBV.

INTRODUCTION

Epstein–Barr virus (EBV) is a human herpesvirus that infects lymphoid and epithelial cells. Although EBV infection is commonly asymptomatic, infection by this virus also causes infectious mononucleosis (Diehl *et al.*, 1968) and is closely associated with many neoplastic disorders (Einhorn *et al.*, 1970; Gunven *et al.*, 1970; Johansson *et al.*, 1970; Klein *et al.*, 1970). Although EBV typically remains latent after infection of B lymphocytes, the virus must enter a lytic cycle to produce virus particles. During the onset of the lytic cycle, the virus expresses the proteins Rta and Zta, encoded by *BRLF1* and *BZLF1*, respectively, to activate the genes required for the viral lytic cycle (Chevallier-Greco *et al.*, 1986; Chiu *et al.*, 2007; Feederle *et al.*, 2000; Granato *et al.*, 2006; Hardwick *et al.*, 1988; Lu *et al.*, 2006). Although the exact means by which the EBV lytic cycle is activated *in vivo* is unknown, activation *in vitro* occurs after latently infected cells are exposed to 12-*O*-tetradecanoylphorbol-13-acetate (TPA), calcium ionophores, transforming growth factor (TGF)-β1 or anti-IgG (Daibata *et al.*, 1990; Faggioni *et al.*, 1986; zur Hausen *et al.*, 1978). TPA, anti-IgG and TGF-β1 are known to activate the ERK signal transduction pathway (Fahmi *et al.*, 2000; Fenton & Sinclair, 1999; Gao *et al.*, 2001; Satoh *et al.*, 1999), which ultimately activates transcription of *BZLF1* and the EBV lytic cycle (Borras *et al.*, 1996; Flemington & Speck, 1990).

It is known that EBV must express Zta to activate its lytic genes (Chevallier-Greco *et al.*, 1986; Chiu *et al.*, 2007; Feederle *et al.*, 2000). Earlier studies have established that Rta upregulates transcription of the Zta gene, *BZLF1* (Adamson *et al.*, 2000; Ragoczy *et al.*, 1998; Zalani *et al.*, 1996). This activation is associated with activation of the p38 and JNK signal transduction pathway, causing the phosphorylation of ATF1/2 and the activation of transcription through an ATF1/2 site in the ZII region of the promoter (Adamson *et al.*, 2000). However, the exact means by which Rta activates these signal transduction cascades is unknown. In this study, we used a yeast two-hybrid analysis to show that Rta interacts with BRCA1-associated protein 2 (BRAP2, also known as IMP), a protein that is known to interact with the kinase suppressor of Ras 1 (KSR1) (Matheny *et al.*, 2004). Müller *et al.* (2001) demonstrated that KSR1 functions as a scaffold, providing a platform for the phosphorylation of MEK1/2 and ERK1/2 (Muller *et al.*, 2001; Nguyen *et al.*, 2002; Roy *et al.*, 2002). However, BRAP2 appears to prevent KSR1 from interacting with the cytoplasmic membrane and homo-oligomerization, thus inhibiting the ERK signal transduction pathway (Chen *et al.*, 2008; Matheny & White, 2006; Matheny *et al.*, 2004). This study demonstrated that Rta prevents the binding of BRAP2 to KSR1, activating the ERK signal transduction pathway and the transcription of *BZLF1* to influence the viral lytic cycle.

METHODS

Cell lines and EBV lytic induction. 293 cells infected with maxi-EBV (a mutant EBV that contains an F replicon and can be

maintained in *Escherichia coli*) [293(maxi-EBV) cells] or its mutant derivative, MI-270, which contains a transposon insertion in *BRLF1* (Chiu *et al.*, 2007; Delecluse *et al.*, 1998), were cultured in Dulbecco's modified Eagle's medium supplemented with 10 % fetal calf serum. Cells were treated with 30 ng TPA ml^{-1} and 3 mM sodium butyrate to induce the EBV lytic cycle (Chang & Liu, 2000; Davies *et al.*, 1991; Luka *et al.*, 1979).

Plasmids. A DNA fragment containing the BRAP2 gene was PCR amplified using primers 5′-CGCGGATCCGAATCCATGAGTGTG-TCACTGGTTGTTATCCG-3′ and 5′-CGGGGTACCAAGCTTTC-AGGGATGTCTGTTGCTCTGAAGG-3′, and a human testis cDNA library (BD Clontech) as template. Plasmids pGEX-BRAP2 and pHA-BRAP2 were constructed by inserting this PCR fragment into the *Bam*HI/*Sma*I sites in pGEX-4T1 (Amersham Biosciences) and *Bam*HI/*Kpn*I sites in pcDNA3-HA2, respectively. A plasmid expressing full-length BRAP2 fused to a glutathione *S*-transferase (GST) sequence at the N terminus (pGST-BRAP2) was constructed by inserting the PCR fragment into pENTR3C (Invitrogen) at the *Bam*HI/*Eco*RI sites and transferring this fragment to pDEST27 using the Gateway system (Invitrogen). Plasmids that expressed deleted GST–BRAP2, including BN262, BC399 and B263/398, which contain the BRAP2 regions aa 1–262, 399–600 and 263–398, respectively, were constructed in a similar way. Plasmid pET-Rta contained *BRLF1* transcribed from the T7 promoter (Chang *et al.*, 2004). Plasmids pCMV-R and pCMV-Z contained *BRLF1* and *BZLF1*, respectively, transcribed from the cytomegalovirus immediate-early promoter (Chang *et al.*, 1998; Hung & Liu, 1999). Plasmid pCMV-3 is an empty vector that was used to construct pCMV-R (Chang *et al.*, 1998). Plasmid pHA-Rta is a plasmid that expresses haemagglutinin (HA)-tagged Rta (Chang *et al.*, 2004). Plasmids pHA-RN415, pHA-RN315, pHA-RN190, pHA-R190/315, pHA-RC255, pHA-R255/415, pHA-RC361, pHA-RC416 and pHA-191/415, which express the regions aa 1–415, 1–315, 1–190, 190–315, 255–605, 255–415, 361–605, 416–605 and 191–415 of HA–Rta (Chang *et al.*, 2004), respectively, were constructed to map the regions in Rta that interact with BRAP2. Plasmids pCDNA3-Flag-KSR1 (Zhang *et al.*, 1997) and pSG/RNLSm (Hsu *et al.*, 2005) express Flag-tagged KSR1 (Flag–KSR1; obtained from Deborah K. Morrison, NCI-Frederick, MD, USA) and an Rta protein with a mutated nuclear localization signal (NLS; obtained from Tsuey-Ying Hsu, 1 Jen-Ai Rd Section 1, Taipei 100, Taiwan, ROC), respectively. Plasmids pZp-Luc and pNS3 were constructed by inserting the −240 to +38 and −57 to +38 regions of the *BZLF1* promoter into the *Hin*dIII/*Sma*I sites in pGL2-Basic (Promega), respectively.

Yeast two-hybrid screen. Proteins that interacted with Rta were identified using a yeast two-hybrid screen with a bait plasmid, pR476, and a human testis cDNA library, according to a method described elsewhere (Chang *et al.*, 2004).

Binding of Rta to BRAP2 *in vitro*. An *E. coli* BL21(DE3)(pGEX-BRAP2) lysate was prepared and a GST pull-down assay was performed as described previously (Chang *et al.*, 2004). Glutathione–Sepharose 4B beads (Amersham Biosciences) were then added to the lysate to allow the binding of GST–BRAP2 to the beads. The beads (30 μl) were then added to an *E. coli* BL21(DE3)(pET-Rta) lysate (500 μl) or a lysate prepared from 293T cells transfected with a plasmid expressing Rta or its deletion derivatives. The reaction mixture was incubated on ice for 1 h. After the beads had been washed in RIPA buffer, electrophoresis sample buffer was added to elute the proteins from the beads by heating at 95 °C for 5 min. Rta was finally detected by immunoblotting. His–Rta was purified from *E. coli* BL21(DE3)(pET-Rta) and bound to Ni-NTA agarose beads (Qiagen). The beads were added to the *E. coli* BL21(DE3)(pGEX-BRAP2) lysate. The binding of GST–BRAP2 to the beads was detected by immunoblotting with anti-GST antibody.

Competitive binding of Rta and KSR1 to BRAP2. 293T cells (5×10^6) were transfected with 4 μg pGST-BRAP2, pCMV-R (0, 3, 6 or 12 μg) and 4 μg pCDNA3-Flag-KSR1. After 24 h of culture, lysates (500 μl) were prepared from the cells using a RIPA buffer without Triton X-100 and sodium deoxycholate. Glutathione–Sepharose beads (30 μl) were then added to the lysate prepared from cells that had been transfected with pGST-BRAP2. The mixture was mixed at 4 °C for 1 h. The beads were washed in RIPA buffer and then mixed with lysate from cells that had been transfected with pCMV-R. After they had been mixed and washed, the beads were finally mixed with lysate from cells that had been transfected with pCDNA3-Flag-KSR1. Glutathione–Sepharose beads were also added to a mixture that contained 500 μl each of the lysates from 293T cells transfected with 4 μg pGST-BRAP2 and pCDNA3-Flag-KSR1. His–Rta, purified from *E. coli* BL21(DE3)(pET-Rta), was then added to the lysate mixture. Proteins that were bound to the beads were eluted with electrophoresis sample buffer and analysed by immunoblotting.

Immunoprecipitation. 293(maxi-EBV) cells (5×10^6) were treated with TPA and sodium butyrate to induce the EBV lytic cycle. Co-immunoprecipitation of Rta and BRAP2 was performed with anti-Rta (1 : 500 dilution) (Argene) and mouse polyclonal anti-BRAP2 antibody (1 : 5000 dilution) as described previously (Chang *et al.*, 2004). Immunoblotting was subsequently conducted to identify the co-immunoprecipitated proteins.

Indirect immunofluorescence analysis. 293(maxi-EBV) cells were transfected with pCMV-Z or treated with TPA and sodium butyrate for 24 h to induce expression of Rta. Cells were collected by centrifugation, plated on poly-L-lysine (Sigma)-coated coverslips and fixed with 4 % paraformaldehyde in PBS at 4 °C for 30 min. The cells were then incubated with anti-Rta monoclonal antibody (mAb) and rabbit anti-BRAP2 polyclonal antibody for 1 h, followed by Alexa Fluor 488-conjugated goat anti-mouse IgG polyclonal antibody and Alexa Fluor 594-conjugated goat anti-rabbit IgG polyclonal antibody (Molecular Probes). After 1 h of incubation, cells were stained with 4′,6-diamidino-2-phenylindole (DAPI). Finally, cells were washed in PBS, mounted in Citifluor (Agar Scientific) and examined under a confocal laser-scanning microscope (model LSM 510 META; Zeiss). The rabbit anti-BRAP2 antibody was produced using synthesized pepticle (KLPSRKGRSKRGK).

Activation of the ERK signal transduction pathway by Rta. 293T cells transfected with pCMV-R were lysed using electrophoresis sample buffer 24 h after transfection. Proteins in the lysate were detected by immunoblotting. U0126 (10 μM; Cell Signalling) was added 4 h prior to lysate preparation to inhibit the ERK signal transduction pathway.

Immunoblot analysis. Proteins were detected by immunoblotting as described previously (Chang *et al.*, 2004). Proteins on the membrane were detected using primary antibodies and horseradish peroxidase-conjugated secondary antibodies, and visualized using SuperSignal West Pico Chemiluminescent substrate (Pierce). Anti-HA was purchased from Roche and anti-α-tubulin and anti-Flag mAbs from Sigma. Anti-β-actin mAb was purchased from Novus Biologicals. Rabbit anti-ERK1/2, anti-phospho-ERK1/2 (Thr202/Tyr204), anti-MEK1/2 and anti-phospho-MEK1/2 (Ser217/221) antibodies were purchased from Cell Signaling Technology. Rabbit anti-GST antibody was purchased from Santa Cruz Biotechnology. Mouse anti-Zta mAb was purchased from Argene. Anti-EA-D mAb was purchased from Millipore. Anti-BRAP2 antibody was produced in mice with bacterially expressed GST–BRAP2.

Transient transfection assay. Plasmids (800 ng) were transfected into 1.5×10^5 293T cells using Lipofectamine 2000 (Invitrogen). Luciferase activity was measured using a luminometer (model LB593; Berthod) as described previously (Chang *et al.*, 1998). Each sample

was prepared in duplicate and each transfection experiment was repeated three times. The copy number of plasmids transfected into cells was determined by real-time PCR using a set of primers specific for the ampicillin-resistance gene (Chang & Liu, 2000). Luciferase activity was normalized to the copy numbers of plasmids.

RESULTS

Interaction between Rta and BRAP2 in yeast and *in vitro*

A yeast two-hybrid screen was performed using a bait plasmid, pR476 (Chang *et al.*, 2004), to screen a human testis cDNA library. A total of 6×10^5 transformants was screened and 10 cellular proteins that interacted with Rta were identified. Sequencing analysis revealed that one of these proteins was BRAP2. A GST pull-down assay was subsequently performed using bacterially expressed GST and GST–BRAP2. GST or GST–BRAP2 bound to glutathione–Sepharose beads was mixed with lysate prepared from *E. coli* BL21(DE3)(pET-Rta) to confirm the interaction. After washing, proteins bound to the beads were eluted and analysed by immunoblotting with anti-Rta antibody. The results revealed that His–Rta in the lysate (Fig. 1a, lane 1) was pulled down by GST–BRAP2–glutathione–Sepharose beads (Fig. 1a, lane 3) but not by GST–glutathione–Sepharose beads (Fig. 1a, lane 2). In another set of experiments, His–Rta bound to Ni-NTA agarose beads was mixed with *E. coli* BL21(DE3)(pGEX-4T1) or *E. coli* BL21(DE3)(pGEX-BRAP2) lysate. Immunoblot analysis indicated that His–Rta bound to Ni-NTA agarose beads retained GST–BRAP2 in the *E. coli* BL21(DE3)(pGEX-BRAP2) lysate (Fig. 1b, lane 4). The binding was not caused by an interaction between GST–BRAP2 and the His tag in His–Rta, as an unrelated His-tagged protein, His–FenB (Lin *et al.*, 1998), did not interact with GST–BRAP2 (data not shown). A negative control also indicated that the His–Rta–Ni-NTA agarose beads did not pull down GST (Fig. 1b, lane 3).

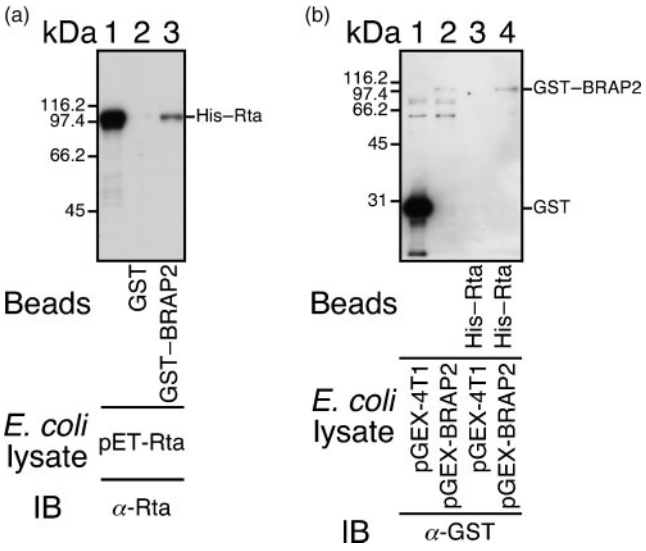

Fig. 1. Interaction between Rta and GST–BRAP2 *in vitro*. (a) An *E. coli* BL21 DE3(pET-Rta) lysate was added to GST and GST–BRAP2 bound to glutathione–Sepharose beads. Proteins bound to the beads were extracted and analysed by immunoblotting (IB) with anti-Rta antibody. Lane 1 was loaded with the *E. coli* BL21(DE3)-(pET-Rta) lysate. (b) Lysates prepared from *E. coli* BL21(DE3)-(pGEX4T-1) (lanes 1 and 3) and *E. coli* BL21(DE3)(pGEX-BRAP2) (lanes 2 and 4) were added to His–Rta–Ni-NTA agarose beads. Proteins bound to the beads were extracted and detected by IB using anti-GST antibody. Lane 1 in (a) and lanes 1 and 2 in (b) were loaded with 0.05 % of the cell lysate.

Interaction between BRAP2 and Rta *in vivo*

293(maxi-EBV) cells were treated with TPA and sodium butyrate to induce the expression of Rta. Immunoblot analysis indicated that Rta in the lysate (Fig. 2a, lane 1) was immunoprecipitated by anti-Rta antibody (Fig. 2a, lane 3) and co-immunoprecipitated with BRAP2 by anti-BRAP2 antibody (Fig. 2a, lane 4) but not by anti-Flag antibody (Fig. 2a, lane 2). Additionally, BRAP2 in the lysate (Fig. 2b, lane 1) was immunoprecipitated by anti-BRAP2 antibody (Fig. 2b, lane 3) and co-immunoprecipitated with Rta by anti-Rta antibody (Fig. 2b, lane 4) but not by anti-Flag antibody (Fig. 2b, lane 2). These results showed that BRAP2 interacts with Rta in 293(maxi-EBV) cells.

Subcellular localization of Rta and BRAP2

Immunofluorescence analysis of 293(maxi-EBV) cells was performed with confocal microscopy to locate Rta and BRAP2. Following lytic induction with TPA and sodium

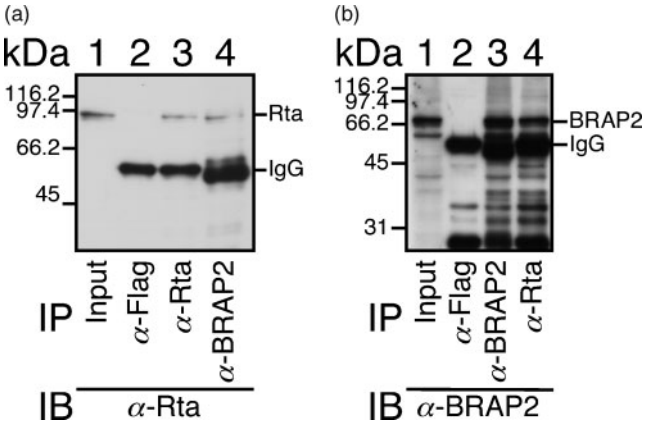

Fig. 2. Co-immunoprecipitation of Rta and BRAP2. Anti-BRAP2, anti-Rta and anti-Flag antibodies were added to the lysate prepared from 293(maxi-EBV) cells treated with TPA and sodium butyrate. Proteins immunoprecipitated (IP) by the antibody were analysed by immunoblotting (IB) with anti-Rta antibody (a) or anti-BRAP2 antibody (b). Lane 1 in (a) was loaded with 0.1 % of the cell lysate, whilst lane 1 in (b) was loaded with 2 % of the cell lysate.

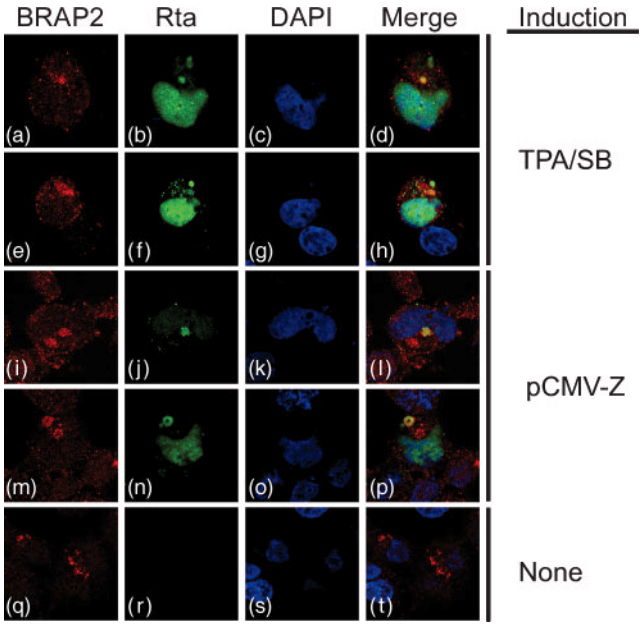

Fig. 3. Indirect immunofluorescence analysis. 293(maxi-EBV) cells were treated with TPA and sodium butyrate (SB) (a–h) or transfected with pCMV-Z (i–p) to activate the EBV lytic cycle. Cells that were not treated with TPA and sodium butyrate or were not transfected with pCMV-Z are shown in (q)–(t). Cells were incubated with rabbit anti-BRAP2 polyclonal antibody (a, e, i, m and q; red) and anti-Rta mAb (b, f, j, n and r; green). DAPI staining (c, g, k, o and s; blue) revealed the positions of the nucleus. Cells were examined under a confocal laser-scanning microscope. Merged images are also shown (d, h, l, p and t).

butyrate, Rta was detected in the cytoplasm and nucleus (Fig. 3b and f). However, BRAP2 was detected only in the cytoplasm (Fig. 3a and e). Merged images showed that Rta and BRAP2 were co-localized in the cytoplasm (Fig. 3d and h). Similar co-localization was also observed in cells transfected with pCMV-Z (Fig. 3i–p), but not in cells that were latently infected by EBV (Fig. 3q–t).

Mapping the interaction domains in BRAP2, KSR1 and Rta

Plasmids expressing HA–Rta and its deletion derivatives (Fig. 4a) were transfected into 293T cells and lysates were prepared. Immunoblot analysis of these lysates confirmed that these proteins were expressed (Fig. 4b). GST–BRAP2–glutathione–Sepharose beads were then added to the lysates. Immunoblot analysis using anti-HA antibody indicated that the beads pulled down HA–Rta, HA–RN415, HA–RN315, HA–RN190, HA–RC255 and HA–RC416 (Fig. 4c, lanes 1–4, 6 and 8), indicating that the regions aa 1–190 and 416–605 in Rta interacted with BRAP2. However, the beads did not pull down proteins that contained the Rta regions aa 191–315 (HA–R191/315) and 255–415 (HA–R255/415) (Fig. 4c, lanes 5 and 7). Additionally, as expected, GST–glutathione–Sepharose beads did not pull down any of these Rta proteins (data not shown). A similar experiment with a GST fusion protein containing full-length or a segment of BRAP2 (Fig. 4e, lanes 2–5) revealed that Rta was pulled down by GST–BRAP2 (Fig. 4d, e, lane 8) and GST–BC399 bound to glutathione–Sepharose beads (Fig. 4d, e, lane 11). However, Rta was not pulled down by GST–BN262 or GST–B263/398 bound to glutathione–Sepharose beads (Fig. 4d), which contained the regions aa 1–262 (Fig. 4e, lane 9) and 263–398 (Fig. 4e, lane 10), respectively. Furthermore, KSR1, which was expressed from pCDNA3-Flag-KSR1 in 293T cells (Fig. 4f, lane 6), was pulled down by GST–BRAP2 and GST–BC399 bound to glutathione–Sepharose beads (Fig. 4f, lanes 8 and 11) but not by GST–BN262 or GST–B263/398 bound to glutathione–Sepharose beads (Fig. 4f, lanes 9 and 10). These results demonstrated that both Rta and KSR1 interacted with GST–BC399.

Competitive binding of Rta and BRAP2 to KSR1

As Rta and KSR1 both interact with the C-terminal 202 aa region in BRAP2, we investigated whether Rta and KSR1 compete for the same binding sites in BRAP2. GST–BRAP2–glutathione–Sepharose beads were incubated with 293T lysates from cells that had been transfected with various amounts of pCMV-R to enable the binding of Rta to the beads. The beads were then incubated with a 293T lysate that contained Flag–KSR1 to determine how Rta affected the binding of Flag–KSR1 to BRAP2. Immunoblot analysis indicated that GST–BRAP2–glutathione–Sepharose beads pulled down KSR1 (Fig. 5a, lane 3). However, GST–glutathione–Sepharose beads did not pull down KSR1 (Fig. 5a, lane 2), confirming that KSR1 interacts with BRAP2. The binding of Flag–KSR1 to GST–BRAP2 was reduced by pre-incubating the GST–BRAP2–glutathione–Sepharose beads in lysate from cells transfected with 3 μg pCMV-R (Fig. 5a, lane 4). Pre-incubating the beads in lysate from cells transfected with 6 or 12 μg pCMV-R further reduced the binding of Flag–KSR1 to BRAP2 to a level that was undetectable by immunoblotting (Fig. 5a, lanes 5 and 6), indicating that Rta impeded the binding of Flag–KSR1 to BRAP2. Meanwhile, in a similar study, two lysates prepared from 293T cells that had been transfected separately with pCDNA3-Flag-KSR1 and pGST-BRAP2 were mixed in equal volumes. After adding glutathione–Sepharose beads, His–Rta purified from an *E. coli* lysate was then added to the lysate mixture. Concentrations up to 0.1 μM bacterially expressed His–Rta did not affect the interaction between Flag–KSR1 and GST–BRAP2 and binding of the proteins to glutathione–Sepharose beads (Fig. 5b, lanes 3–5), whilst adding 0.3 μM His–Rta decreased the amount of Flag–KSR1 that was retained by the beads (Fig. 5b, lane 6), showing that Rta dislodges KSR1 from BRAP2.

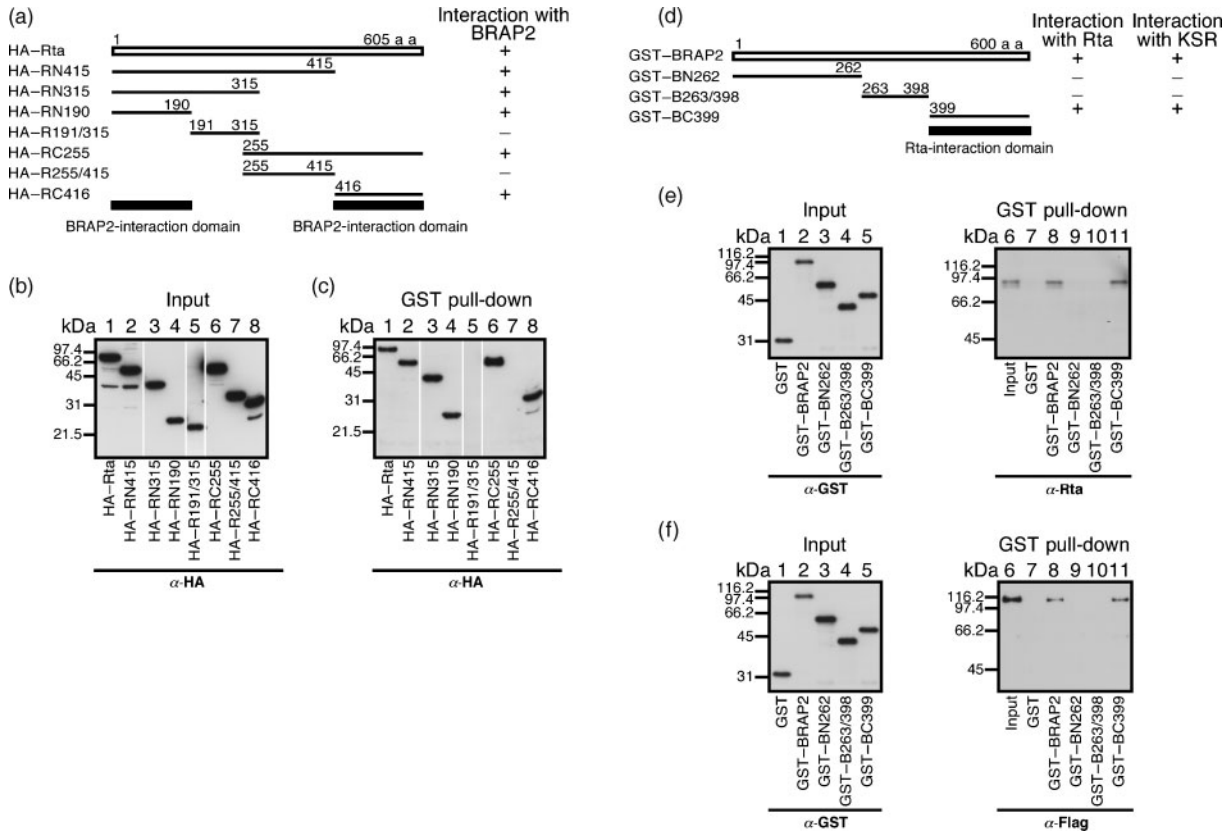

Fig. 4. Mapping of the interaction domains in Rta, BRAP2 and KSR1. Plasmids expressing HA-tagged Rta (HA–Rta) and its deletion derivatives (a) were transfected into 293T cells. Proteins in the lysates were analysed by immunoblotting with anti-HA antibody (b). Proteins that were pulled down by GST–BRAP2–glutathione–Sepharose beads were analysed by immunoblotting with anti-HA antibody (c). The regions in BRAP2 that interacted with Rta and KSR1 were analysed in a similar way. GST fusion proteins containing full-length or a segment of BRAP2 (d) bound to glutathione–Sepharose beads were added to lysates prepared from 293T cells that had been transfected with pCMV-R (e) or pCDNA3-Flag-KSR1 (f). Lanes 1 and 6 in (e) and (f) were loaded with the cell lysate.

Activating the ERK signal transduction pathway by Rta

As Rta prevents BRAP2 from binding to KSR1, Rta may eliminate the inhibition of the ERK signal transduction pathway by BRAP2. Immunoblot analysis indicated that transfecting 0.5–2 μg pCMV-R into 293T cells did not change the overall level of MEK1/2 and ERK1/2 in the cell (Fig. 6a, lanes 2–4, 6 and 8), but promoted the phosphorylation of MEK1/2 and ERK1/2 (Fig. 6a, lanes 1–4). Additionally, adding U0126, which inhibits the activity of MEK1/2, prevented the phosphorylation of ERK1/2 activated by Rta and the Rta NLS mutant (Fig. 6a, lanes 6 and 7). We also found that transfecting pHA-BRAP2 inhibited the phosphorylation of MEK1/2 and ERK1/2 activated by Rta and the Rta NLS mutant (Fig. 6a, lanes 8 and 9). A similar study was also performed using BJAB, Akata, EBV-negative Akata and P3HR1 cells; the activation of ERK1/2 phosphorylation by Rta in these cell lines was less obvious than that in 293T cells (data not shown).

Activation of ERK1/2 by the BRAP2-interacting domains in Rta

We also studied whether the expression of two Rta fragments that bind to BRAP2, HA–RN190 (Fig. 4a) and HA–RC361 (a protein that contains the C-terminal region of Rta from aa 361–605), influenced the phosphorylation of ERK1/2. Immunoblot analysis indicated that, although transfecting a plasmid expressing HA–R191/415, which does not interact with BRAP2, had little effect on the phosphorylation of ERK1/2 (Fig. 6b, lane 4), transfecting a plasmid that expressed HA–RC361 increased the phosphorylation level of ERK1/2 (Fig. 6b, lane 5). Similar activation was also observed upon transfection of a plasmid that expressed HA–RN190 (Fig. 6b, lane 3). Co-expressing HA–RN190 and HA–RC361 also increased the phosphorylation levels of MEK1/2 and ERK1/2 (Fig. 6b, lane 6). Furthermore, similar activation was also observed after co-expressing HA–RN190 and HA–RN416 (Fig. 4a and data not shown). The addition of U0126 did not prevent the phosphorylation of MEK1/2, but inhibited the phosphor-

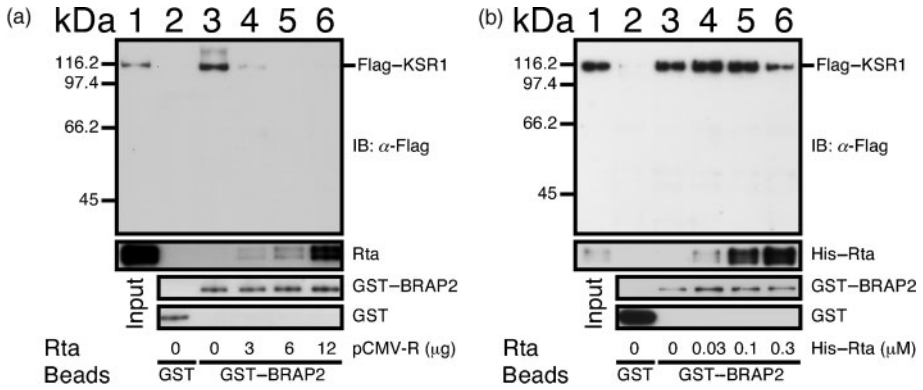

Fig. 5. Inhibition of binding of BRAP2 to KSR1 by Rta. (a) Glutathione–Sepharose beads were added to the lysate prepared from 5×10^6 293T cells transfected with 4 μg pGST–BRAP2 (lanes 3–6) to enable the binding of GST–BRAP2 to the beads. The beads were washed and mixed with 500 μl of a lysate prepared from the same number of 293T cells transfected with 0, 3, 6 or 12 μg pCMV-R (lanes 3–6). The beads were finally mixed with a lysate prepared from 5×10^6 293T cells transfected with pCDNA3-Flag-KSR1. (b) Lysates (500 μl) containing GST–BRAP2 and Flag–KSR1 were mixed. Glutathione–Sepharose beads and His–Rta were subsequently added to the lysate mixture as indicated. In (a) and (b), Flag-tagged KSR1 bound to the beads was extracted and examined by immunoblotting (IB) with anti-Flag antibody. GST–glutathione–Sepharose beads were also used to demonstrate the lack of binding between GST and KSR1 (lane 2). Lane 1 was loaded with 0.02 % of the lysate. Flag–KSR1 and Rta bound to GST–BRAP2–glutathione–Sepharose beads were detected with anti-Flag and anti-Rta antibody, respectively; GST and GST–BRAP2 were detected with anti-GST antibody.

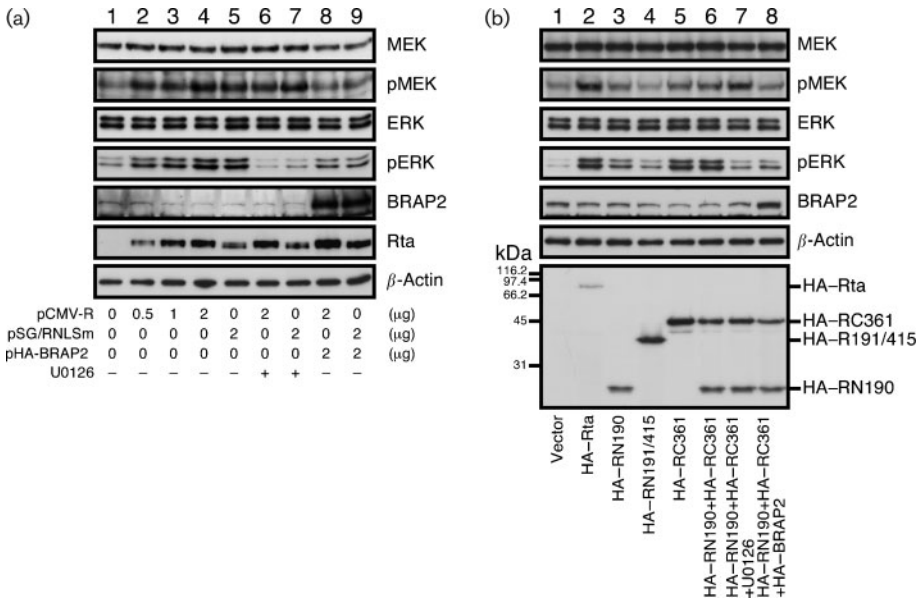

Fig. 6. Activation of the ERK signal transduction pathway by Rta and its fragments. Lysates were prepared from 293T cells transfected with 0–2 μg pCMV-R (a) or plasmids expressing HA-tagged Rta and its deletion derivatives (b). Cells transfected with an empty vector, pcDNA3-HA2, were used as a negative control. MEK1/2 (MEK), phosphorylated MEK1/2 (pMEK), ERK1/2 (ERK), phosphorylated ERK1/2 (pERK), Rta, BRAP2 and β-actin in the lysate were detected by immunoblotting with their respective antibodies. U0126 in DMSO was used to inhibit the function of MEK1/2. Plasmid pSG/RNLSm expressed a mutant Rta protein lacking the NLS. Expression of HA–Rta, HA–RC361, HA–RN190 and HA–RN191/415 was examined by immunoblotting using anti-HA antibody.

ylation of ERK1/2 activated by HA–RN190 and HA–RC361 (Fig. 6b, lanes 6 and 7). This study also found that expressing BRAP2 inhibited MEK and ERK phosphorylation activated by HA–RN190 and HA–RC361 (Fig. 6b, lane 8).

Activation of the *BZLF1* promoter by Rta

Previous studies have established that *BZLF1* transcription is closely associated with activation of the ERK signal transduction cascade (Fahmi *et al.*, 2000; Fenton & Sinclair, 1999; Satoh *et al.*, 1999). To determine whether Rta activates *BZLF1* transcription via the ERK signal transduction pathway, pCMV-R and a *BZLF1* reporter plasmid, pZp-Luc, were co-transfected into 293T cells. The *BZLF1* promoter was activated by pCMV-R at a level about 10-fold higher than that achieved by pCMV-3 (Fig. 7a and b). Adding U0126 reduced the promoter activity by 56 % (Fig. 7a), suggesting that activation of the ERK signal transduction pathway by Rta is important for the transcription of *BZLF1*. Additionally, pNS3, in which the four TPA-response elements (TREs) and the ZII region in the *BZLF1* promoter were deleted, was not activated by pCMV-R, indicating that TREs may be associated with the activation. However, transfecting a plasmid expressing HA–RN190 or HA–RC416 also activated *BZLF1* transcription from pZp-Luc by 2.2-fold or 1.6-fold, respectively (Fig. 7b). Transfecting plasmids that expressed both fragments increased the promoter activity 3.3-fold (Fig. 7b). Adding U0126 inhibited transcription to the basal level, indicating the importance of Rta-induced ERK signal transduction in activating the transcription of *BZLF1*.

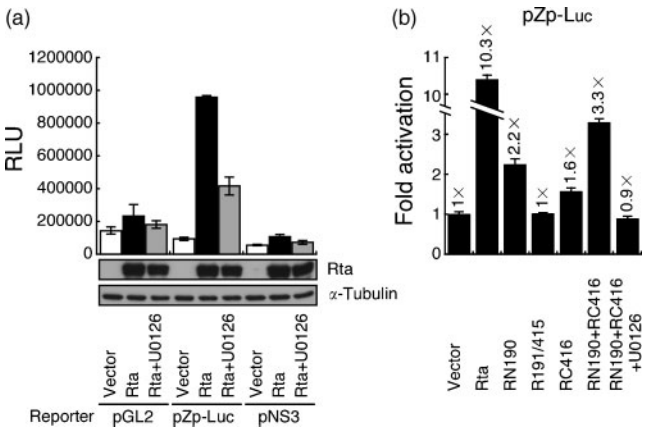

Fig. 7. Activation of the *BZLF1* promoter by Rta and its domains that interact with BRAP2. (a) Reporter plasmids pGL2-Basic (pGL2), pZp-Luc and pNS3 were co-transfected with pCMV-3 (vector) or pCMV-R (Rta) into 293T cells. The amount of Rta in the lysate was determined by immunoblotting (bottom panel). (b) pZp-Luc was co-transfected with pcDNA3-HA2 (vector), pCMV-R, pHA-RN190, pHA-R191/415 and pHA-RC416 into 293T cells. The copy number of plasmids that were transfected into the cells was determined by real-time PCR using a set of primers specific for the ampicillin-resistance gene. The luciferase activity was normalized to the copy number of the plasmids to determine the fold activation. U0126 was added to inhibit the ERK signal transduction cascade. Luciferase activity was measured at 24 h after transfection. Each sample was prepared in duplicate and each experiment was repeated three times. RLU, Relative light units.

Activation of EBV lytic genes by Rta via the ERK signal transduction pathway

To demonstrate that activation of the ERK signalling pathway by Rta is critical to the EBV lytic activation, we transfected pCMV-R into 293 cells infected by a maxi-EBV mutant strain, MI-270, containing a mutated *BRLF1* (Chiu *et al.*, 2007). Immunoblotting revealed that the transfection increased the expression levels of Zta and diffused early antigen (EA-D) (Fig. 8, lanes 2 and 3). Adding U0126, however, significantly lowered the level of Zta and EA-D expression, indicating that activation of the ERK signal transduction pathway by Rta is crucial for activation of the EBV lytic cycle.

DISCUSSION

Rta is known to interact with cellular proteins to affect its own functions or those of the cell. For instance, the interaction with Ubc9 and PIAS1 causes Rta sumoylation, which enhances the transcription activity of Rta (Chang *et al.*, 2004; Liu *et al.*, 2006). The interaction between Rta and Rb releases E2F1 from Rb to affect cell-cycle progression (Swenson *et al.*, 1999; Zacny *et al.*, 1998). Rta also interacts with MCAF1, an Sp1-binding protein, to enhance Sp1-mediated transcription (Chang *et al.*, 2005). This study found that Rta interacts with a KSR1-binding protein, BRAP2. The interaction was confirmed *in vitro* using a GST

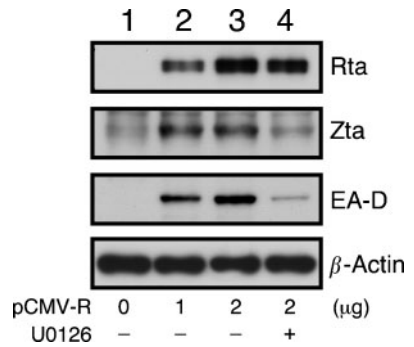

Fig. 8. Inhibition of Rta-induced Zta and EA-D expression by U0126. Plasmid pCMV-R was transfected into 293T cells infected by a mutant maxi-EBV strain, MI-270, which contained a mutated *BRLF1*. Expression of Rta, Zta, EA-D and β-actin was determined by immunoblot analysis 24 h after transfection. U0126 was added to inhibit the ERK signal transduction pathway.

pull-down assay (Fig. 1) and *in vivo* by co-immunoprecipitation (Fig. 2). Confocal microscopy showed that Rta and BRAP2 co-localized in the cytoplasm (Fig. 3), which is consistent with the knowledge that BRAP2 is a cytoplasmic protein (Asada *et al.*, 2004; Li *et al.*, 1998).

As BRAP2 interacts with the NLS in BRCA1 and p21 to retain these two proteins in the cytoplasm (Asada *et al.*, 2004; Li *et al.*, 1998), we investigated whether expression of BRAP2 also retained Rta in the cytoplasm. To accomplish this, 293(maxi-EBV) cells were transfected with pHA-BRAP2 and treated with TPA and sodium butyrate. Confocal microscopy revealed that, although BRAP2 was expressed abundantly in the cell, the expression did not affect the localization of Rta and its ability to transactivate a promoter containing an Rta-response element (data not shown), showing that BRAP2 probably does not retain Rta in the cytoplasm to affect its nuclear functions. BRAP2 is also a ubiquitin E3 ligase (Matheny *et al.*, 2004; Pai *et al.*, 2007). However, we found that Rta, although conjugated by SUMO-1 (Chang *et al.*, 2004), was not conjugated by ubiquitin (unpublished results), suggesting that BRAP2 does not influence the function of Rta via ubiquitination. Another important function of BRAP2 is its ability to bind to KSR1 to inhibit ERK signal transduction (Chen *et al.*, 2008; Matheny *et al.*, 2004). KSR1 is a scaffolding protein that facilitates the phosphorylation of MEK1/2 and ERK1/2 in the ERK signal transduction cascade (Muller *et al.*, 2001; Nguyen *et al.*, 2002; Roy *et al.*, 2002). However, BRAP2 prevents KSR1 homo-oligomerization and prevents it from associating with the cytoplasmic membrane to inhibit ERK signal transduction (Chen *et al.*, 2008; Matheny *et al.*, 2004). Therefore, we investigated whether Rta influenced the capacity of BRAP2 to inhibit ERK signal transduction. A mapping study found that Rta and KSR1 both interacted with the C-terminal 202 aa region in BRAP2 (Fig. 4). Thus, we suggest that Rta binds to BRAP2 to prevent the interaction between BRAP2 and KSR1, which activates the ERK signal transduction cascade. Furthermore, Rta activates the *BZLF1* promoter through an ATF2 site in the ZII region (Adamson *et al.*, 2000). Therefore, activation of the ERK signal transduction pathway by Rta may ultimately influence the transcription of *BZLF1* through the activation of ATF2, a downstream target of the ERK signal transduction pathway (Morton *et al.*, 2004; Ouwens *et al.*, 2002). The first piece of evidence in support of this hypothesis is the fact that the binding capacity of GST–BRAP2–glutathione–Sepharose beads to KSR1 declined substantially when the beads were pre-incubated with cell lysates containing Rta (Fig. 5a); adding bacterially expressed His–Rta to a lysate mixture containing Flag–KSR1 and GST–BRAP2 also dislodged Flag–KSR1 from the GST–BRAP2–glutathione–Sepharose beads (Fig. 5b), indicating that Rta prevents the interaction between BRAP2 and KSR1. Secondly, the results of the immunoblot analysis showed that transfecting 293T cells with pCMV-R increased the degree of phosphorylation of MEK1/2 and ERK1/2 (Fig. 6a). Finally, previous studies have established that TPA, anti-IgG and TGF-β1 activate *BZLF1* transcription through the four TREs and the ZII region in the *BZLF1* promoter (Adamson *et al.*, 2000; Fenton & Sinclair, 1999; Ragoczy *et al.*, 1998; Satoh *et al.*, 1999). A transient transfection study revealed that the capacity of Rta to activate the mutant *BZLF1* promoter without these sites (pNS3) was reduce substantially (Fig. 7a). Additionally, the fact that Rta-activated *BZLF1* transcription is inhibited by U0126 (Fig. 7a) also supports the suggestion that Rta activates transcription via activation of the ERK signal transduction pathway. Notably, transient transfection analysis indicated that U0126 did not completely repress Rta-activated *BZLF1* transcription (Fig. 7a), which is probably due to the fact that Rta also activates *BZLF1* transcription via the p38 and JNK pathway (Adamson *et al.*, 2000), and activation via these routes was unaffected by the U0126 treatment. We also found that expressing the two domains in Rta that interact with BRAP2 sufficiently increased the degree of phosphorylation of MEK1/2 and ERK1/2 (Fig. 6b) and activated the *BZLF1* promoter (Fig. 7b). Unlike intact Rta, transactivation of the *BZLF1* promoter was completely inhibited by U0126 (Fig. 7b), implying that, unlike the full-length Rta, these two Rta fragments are not involved in activating the p38 and JNK signalling pathway to activate *BZLF1* transcription. Previous studies have demonstrated that activation of ERK signal transduction by TPA, anti-IgG and TGF-β1 is crucial to activation of *BZLF1* transcription and the EBV lytic cycle (Fahmi *et al.*, 2000; Fenton & Sinclair, 1999; Satoh *et al.*, 1999). The fact that U0126 reduced the capacity of Rta to activate expression of Zta and EA-D (Fig. 8) indicates that activation of the ERK signal transduction pathway by Rta is critical to EBV reactivation. Our results also explain why an NLS mutant of Rta was found previously to activate the EBV lytic cycle (Hsu *et al.*, 2005).

This investigation found that Rta did not promote the phosphorylation of ERK1/2 in three B-lymphocyte cell lines (Akata, BJAB and P3HR1) as much as in 293T cells (data not shown). There is a possibility that the ERK signal transduction pathway in these B lymphocyte cells is less responsive to BRAP2 inhibition, so Rta does not significantly activate the pathway in such cells. Earlier studies have demonstrated that Zta also activates the *BRLF1* promoter by activating the ERK signal transduction cascade in epithelial cells (Chang *et al.*, 2006), showing that both Rta and Zta influence ERK signal transduction to influence the EBV lytic cycle. As the EBV particles produced by epithelial cells exhibit a tropism towards B lymphocytes (Borza & Hutt-Fletcher, 2002; Guerreiro-Cacais *et al.*, 2004), in which EBV latency is established, activation of the *BZLF1* promoter by Rta through the ERK signal transduction pathway may be critical to viral lytic replication and to the infection of B lymphocytes in the B-lymphocyte/epithelial cell infection cycle.

ACKNOWLEDGEMENTS

The authors would like to thank Deborah K. Morrison and Tsuey-Ying Hsu for providing the plasmids used in this study. This research was supported by the National Science Council of the Republic of China (NSC96-3112-B-182-002 and NSC95-2320-B-182-041-MY3), the National Health Research Institute of the Republic of China (NHRI-EX96-9417BI) and the Chang-Gung Molecular Medicine Research Center (CMRPD160111).

REFERENCES

Adamson, A. L., Darr, D., Holley-Guthrie, E., Johnson, R. A., Mauser, A., Swenson, J. & Kenney, S. (2000). Epstein–Barr virus immediate-early proteins BZLF1 and BRLF1 activate the ATF2 transcription factor by increasing the levels of phosphorylated p38 and c-Jun N-terminal kinases. *J Virol* **74**, 1224–1233.

Asada, M., Ohmi, K., Delia, D., Enosawa, S., Suzuki, S., Yuo, A., Suzuki, H. & Mizutani, S. (2004). Brap2 functions as a cytoplasmic retention protein for p21 during monocyte differentiation. *Mol Cell Biol* **24**, 8236–8243.

Borras, A. M., Strominger, J. L. & Speck, S. H. (1996). Characterization of the ZI domains in the Epstein–Barr virus BZLF1 gene promoter: role in phorbol ester induction. *J Virol* **70**, 3894–3901.

Borza, C. M. & Hutt-Fletcher, L. M. (2002). Alternate replication in B cells and epithelial cells switches tropism of Epstein–Barr virus. *Nat Med* **8**, 594–599.

Chang, L. K. & Liu, S. T. (2000). Activation of the BRLF1 promoter and lytic cycle of Epstein–Barr virus by histone acetylation. *Nucleic Acids Res* **28**, 3918–3925.

Chang, L. K., Lee, Y. H., Cheng, T. S., Hong, Y. R., Lu, P. J., Wang, J. J., Wang, W. H., Kuo, C. W., Li, S. S. & Liu, S. T. (2004). Post-translational modification of Rta of Epstein–Barr virus by SUMO-1. *J Biol Chem* **279**, 38803–38812.

Chang, L. K., Chung, J. Y., Hong, Y. R., Ichimura, T., Nakao, M. & Liu, S. T. (2005). Activation of Sp1-mediated transcription by Rta of Epstein–Barr virus via an interaction with MCAF1. *Nucleic Acids Res* **33**, 6528–6539.

Chang, P. J., Chang, Y. S. & Liu, S. T. (1998). Role of Rta in the translation of bicistronic BZLF1 of Epstein–Barr virus. *J Virol* **72**, 5128–5136.

Chang, Y., Lee, H. H., Chen, Y. T., Lu, J., Wu, S. Y., Chen, C. W., Takada, K. & Tsai, C. H. (2006). Induction of the early growth response 1 gene by Epstein–Barr virus lytic transactivator Zta. *J Virol* **80**, 7748–7755.

Chen, C., Lewis, R. E. & White, M. A. (2008). IMP modulates KSR1-dependent multivalent complex formation to specify ERK1/2 pathway activation and response thresholds. *J Biol Chem* **283**, 12789–12796.

Chevallier-Greco, A., Manet, E., Chavrier, P., Mosnier, C., Daillie, J. & Sergeant, A. (1986). Both Epstein–Barr virus (EBV)-encoded *trans*-acting factors, EB1 and EB2, are required to activate transcription from an EBV early promoter. *EMBO J* **5**, 3243–3249.

Chiu, Y. F., Tung, C. P., Lee, Y. H., Wang, W. H., Li, C., Hung, J. Y., Wang, C. Y., Kawaguchi, Y. & Liu, S. T. (2007). A comprehensive library of mutations of Epstein–Barr virus. *J Gen Virol* **88**, 2463–2472.

Daibata, M., Humphreys, R. E., Takada, K. & Sairenji, T. (1990). Activation of latent EBV via anti-IgG-triggered, second messenger pathways in the Burkitt's lymphoma cell line Akata. *J Immunol* **144**, 4788–4793.

Davies, A. H., Grand, R. J., Evans, F. J. & Rickinson, A. B. (1991). Induction of Epstein–Barr virus lytic cycle by tumor-promoting and non-tumor-promoting phorbol esters requires active protein kinase C. *J Virol* **65**, 6838–6844.

Delecluse, H. J., Hilsendegen, T., Pich, D., Zeidler, R. & Hammerschmidt, W. (1998). Propagation and recovery of intact, infectious Epstein–Barr virus from prokaryotic to human cells. *Proc Natl Acad Sci U S A* **95**, 8245–8250.

Diehl, V., Henle, G., Henle, W. & Kohn, G. (1968). Demonstration of a herpes group virus in cultures of peripheral leukocytes from patients with infectious mononucleosis. *J Virol* **2**, 663–669.

Einhorn, N., Klein, G. & Clifford, P. (1970). Increase in antibody titer against the EBV-associated membrane antigen complex in Burkitt's lymphoma and nasopharyngeal carcinoma after local irradiation. *Cancer* **26**, 1013–1021.

Faggioni, A., Zompetta, C., Grimaldi, S., Barile, G., Frati, L. & Lazdins, J. (1986). Calcium modulation activates Epstein–Barr virus genome in latently infected cells. *Science* **232**, 1554–1556.

Fahmi, H., Cochet, C., Hmama, Z., Opolon, P. & Joab, I. (2000). Transforming growth factor beta 1 stimulates expression of the Epstein–Barr virus BZLF1 immediate-early gene product ZEBRA by an indirect mechanism which requires the MAPK kinase pathway. *J Virol* **74**, 5810–5818.

Feederle, R., Kost, M., Baumann, M., Janz, A., Drouet, E., Hammerschmidt, W. & Delecluse, H. J. (2000). The Epstein–Barr virus lytic program is controlled by the co-operative functions of two transactivators. *EMBO J* **19**, 3080–3089.

Fenton, M. & Sinclair, A. J. (1999). Divergent requirements for the MAPK(ERK) signal transduction pathway during initial virus infection of quiescent primary B cells and disruption of Epstein–Barr virus latency by phorbol esters. *J Virol* **73**, 8913–8916.

Flemington, E. & Speck, S. H. (1990). Identification of phorbol ester response elements in the promoter of Epstein–Barr virus putative lytic switch gene BZLF1. *J Virol* **64**, 1217–1226.

Gao, X., Ikuta, K., Tajima, M. & Sairenji, T. (2001). 12-*O*-tetradecanoylphorbol-13-acetate induces Epstein–Barr virus reactivation via NF-κB and AP-1 as regulated by protein kinase C and mitogen-activated protein kinase. *Virology* **286**, 91–99.

Granato, M., Farina, A., Gonnella, R., Santarelli, R., Frati, L., Faggioni, A. & Angeloni, A. (2006). Regulation of the expression of the Epstein–Barr virus early gene BFRF1. *Virology* **347**, 109–116.

Guerreiro-Cacais, A. O., Li, L., Donati, D., Bejarano, M. T., Morgan, A., Masucci, M. G., Hutt-Fletcher, L. & Levitsky, V. (2004). Capacity of Epstein–Barr virus to infect monocytes and inhibit their development into dendritic cells is affected by the cell type supporting virus replication. *J Gen Virol* **85**, 2767–2778.

Gunven, P., Klein, G., Henle, G., Henle, W. & Clifford, P. (1970). Epstein–Barr virus in Burkitt's lymphoma and nasopharyngeal carcinoma. Antibodies to EBV associated membrane and viral capsid antigens in Burkitt lymphoma patients. *Nature* **228**, 1053–1056.

Hardwick, J. M., Lieberman, P. M. & Hayward, S. D. (1988). A new Epstein–Barr virus transactivator, R, induces expression of a cytoplasmic early antigen. *J Virol* **62**, 2274–2284.

Hsu, T. Y., Chang, Y., Wang, P. W., Liu, M. Y., Chen, M. R., Chen, J. Y. & Tsai, C. H. (2005). Reactivation of Epstein–Barr virus can be triggered by an Rta protein mutated at the nuclear localization signal. *J Gen Virol* **86**, 317–322.

Hung, C. H. & Liu, S. T. (1999). Characterization of the Epstein–Barr virus BALF2 promoter. *J Gen Virol* **80**, 2747–2750.

Johansson, B., Klein, G., Henle, W. & Henle, G. (1970). Epstein–Barr virus (EBV)-associated antibody patterns in malignant lymphoma and leukemia. I. Hodgkin's disease. *Int J Cancer* **6**, 450–462.

Klein, G., Geering, G., Old, L. J., Henle, G., Henle, W. & Clifford, P. (1970). Comparison of the anti-EBV titer and the EBV-associated

membrane reactive and precipitating antibody levels in the sera of Burkitt lymphoma and nasopharyngeal carcinoma patients and controls. *Int J Cancer* **5**, 185–194.

Li, S., Ku, C. Y., Farmer, A. A., Cong, Y. S., Chen, C. F. & Lee, W. H. (1998). Identification of a novel cytoplasmic protein that specifically binds to nuclear localization signal motifs. *J Biol Chem* **273**, 6183–6189.

Lin, G. H., Chen, C. L., Tschen, J. S., Tsay, S. S., Chang, Y. S. & Liu, S. T. (1998). Molecular cloning and characterization of fengycin synthetase gene *fenB* from *Bacillus subtilis*. *J Bacteriol* **180**, 1338–1341.

Liu, S. T., Wang, W. H., Hong, Y. R., Chuang, J. Y., Lu, P. J. & Chang, L. K. (2006). Sumoylation of Rta of Epstein–Barr virus is preferentially enhanced by PIASxβ. *Virus Res* **119**, 163–170.

Lu, C. C., Jeng, Y. Y., Tsai, C. H., Liu, M. Y., Yeh, S. W., Hsu, T. Y. & Chen, M. R. (2006). Genome-wide transcription program and expression of the Rta responsive gene of Epstein–Barr virus. *Virology* **345**, 358–372.

Luka, J., Kallin, B. & Klein, G. (1979). Induction of the Epstein–Barr virus (EBV) cycle in latently infected cells by *n*-butyrate. *Virology* **94**, 228–231.

Matheny, S. A. & White, M. A. (2006). Ras-sensitive IMP modulation of the Raf/MEK/ERK cascade through KSR1. *Methods Enzymol* **407**, 237–247.

Matheny, S. A., Chen, C., Kortum, R. L., Razidlo, G. L., Lewis, R. E. & White, M. A. (2004). Ras regulates assembly of mitogenic signalling complexes through the effector protein IMP. *Nature* **427**, 256–260.

Morton, S., Davis, R. J. & Cohen, P. (2004). Signalling pathways involved in multisite phosphorylation of the transcription factor ATF-2. *FEBS Lett* **572**, 177–183.

Müller, J., Ory, S., Copeland, T., Piwnica-Worms, H. & Morrison, D. K. (2001). C-TAK1 regulates Ras signaling by phosphorylating the MAPK scaffold, KSR1. *Mol Cell* **8**, 983–993.

Nguyen, A., Burack, W. R., Stock, J. L., Kortum, R., Chaika, O. V., Afkarian, M., Muller, W. J., Murphy, K. M., Morrison, D. K. & other authors (2002). Kinase suppressor of Ras (KSR) is a scaffold which facilitates mitogen-activated protein kinase activation in vivo. *Mol Cell Biol* **22**, 3035–3045.

Ouwens, D. M., de Ruiter, N. D., van der Zon, G. C., Carter, A. P., Schouten, J., van der Burgt, C., Kooistra, K., Bos, J. L., Maassen, J. A. & van Dam, H. (2002). Growth factors can activate ATF2 via a two-step mechanism: phosphorylation of Thr71 through the Ras–MEK–ERK pathway and of Thr69 through RalGDS–Src–p38. *EMBO J* **21**, 3782–3793.

Pai, M. T., Tzeng, S. R., Kovacs, J. J., Keaton, M. A., Li, S. S., Yao, T. P. & Zhou, P. (2007). Solution structure of the Ubp-M BUZ domain, a highly specific protein module that recognizes the C-terminal tail of free ubiquitin. *J Mol Biol* **370**, 290–302.

Ragoczy, T., Heston, L. & Miller, G. (1998). The Epstein–Barr virus Rta protein activates lytic cycle genes and can disrupt latency in B lymphocytes. *J Virol* **72**, 7978–7984.

Roy, F., Laberge, G., Douziech, M., Ferland-McCollough, D. & Therrien, M. (2002). KSR is a scaffold required for activation of the ERK/MAPK module. *Genes Dev* **16**, 427–438.

Satoh, T., Hoshikawa, Y., Satoh, Y., Kurata, T. & Sairenji, T. (1999). The interaction of mitogen-activated protein kinases to Epstein–Barr virus activation in Akata cells. *Virus Genes* **18**, 57–64.

Swenson, J. J., Mauser, A. E., Kaufmann, W. K. & Kenney, S. C. (1999). The Epstein–Barr virus protein BRLF1 activates S phase entry through E2F1 induction. *J Virol* **73**, 6540–6550.

Zacny, V. L., Wilson, J. & Pagano, J. S. (1998). The Epstein–Barr virus immediate-early gene product, BRLF1, interacts with the retinoblastoma protein during the viral lytic cycle. *J Virol* **72**, 8043–8051.

Zalani, S., Holley-Guthrie, E. & Kenney, S. (1996). Epstein–Barr viral latency is disrupted by the immediate-early BRLF1 protein through a cell-specific mechanism. *Proc Natl Acad Sci U S A* **93**, 9194–9199.

Zhang, Y., Yao, B., Delikat, S., Bayoumy, S., Lin, X. H., Basu, S., McGinley, M., Chan-Hui, P. Y., Lichenstein, H. & Kolesnick, R. (1997). Kinase suppressor of Ras is ceramide-activated protein kinase. *Cell* **89**, 63–72.

zur Hausen, H., O'Neill, F. J., Freese, U. K. & Hecker, E. (1978). Persisting oncogenic herpesvirus induced by the tumour promotor TPA. *Nature* **272**, 373–375.